

ASTROPHYSICS

PROTON UNBOUND STATES IN T=3/2 AND T=2 NUCLEI AND THE REACTION RATES FOR SEQUENTIAL TWO-PROTON CAPTURE REACTIONS IN THE rp-PROCESS

H. Schatz, J. Görres, H. Herndl, N. Kaloskamis, E. Stech, P. Tischhauser,
and M. Wiescher

University of Notre Dame, Dept. of Physics, Notre Dame, Indiana 46556

A. Bacher, G.P.A. Berg, T.C. Black, S. Choi, C.C. Foster, K. Jiang,
W. Schmitt, and E.J. Stephenson

Indiana University Cyclotron Facility, Bloomington, Indiana 47408

Proton capture reactions on T=1 nuclei (e.g. ^{22}Mg , ^{26}Si , ^{30}S , and ^{34}Ar) are considered the main impedance on the rp-process reaction path^{1,2} below A=46. Low proton-capture Q-values result in large inverse photodisintegration rates at the typical temperature and density conditions in explosive hydrogen burning scenarios. As a consequence most of the processed material remains stored in the T=1 nuclei until they undergo β -decay (waiting points).

It was pointed out³ that a rapid subsequent proton capture on the low abundance T=3/2 nuclei (e.g. ^{23}Al , ^{27}P , ^{31}Cl , and ^{35}K) may bridge these waiting points. This will reduce the timescale of the rp-process considerably and may increase the production rate of heavy elements during explosive hydrogen burning. It will also strongly reduce the final abundances of the T=1 nuclei, which is of particular importance in the case of ^{22}Mg and ^{26}Si , the progenitors of the long lived γ -ray sources ^{22}Na and ^{26}Al .

To study these effects in dynamic nucleosynthesis models, it is necessary to determine the reaction rates for proton capture on T=1 and T=3/2 neutron-deficient nuclei below mass A=46. The resonant reaction rate for proton-capture processes as a function of temperature T_9 (in units of GK),

$$N_A \langle \sigma v \rangle = 1.504 \cdot 10^{11} (\mu \cdot T_9)^{-1/3} \sum_i \omega \gamma_i \cdot \exp\left(\frac{-11.605 \cdot E_i}{kT_9}\right),$$

depends linearly on the resonance strength $\omega \gamma_i$ (in MeV) and exponentially on the resonance energy E_i (in MeV). The resonance strengths can be calculated reliably for sd-shell nuclei using large configuration-space shell-model calculations. The major uncertainty in the resulting reaction rates is the uncertainty in the predicted resonance energies of typically ± 100 keV or more. This results in reaction-rate uncertainties of several orders of magnitude.

Experiment E389 was proposed to measure the energies of low lying proton unbound states in $T=3/2$ and $T=2$ nuclei. The $T=3/2$ and $T=2$ isotopes can be studied using the ($^3\text{He}, ^8\text{Li}$) reaction and the ($^4\text{He}, ^8\text{He}$) reaction on $T=0$ target nuclei, respectively.

In a first step we concentrated on the two reaction sequences $^{22}\text{Mg}(p,\gamma)^{23}\text{Al}(p,\gamma)^{24}\text{Si}$ and $^{26}\text{Si}(p,\gamma)^{27}\text{P}(p,\gamma)^{28}\text{S}$, specifically on the measurement of proton unbound states in ^{24}Si and ^{28}S populated via the $^{28}\text{Si}(\alpha, ^8\text{He})^{24}\text{Si}$ and $^{32}\text{S}(\alpha, ^8\text{He})^{28}\text{S}$ reactions respectively.

A first test run for the ^{24}Si experiment was performed in July 1995 with a 200-MeV, 500-nA α -beam on a natural Si target. The reaction products were momentum analyzed with the K600 spectrograph in the septum mode at 4.5° . The focal plane detector system consisted of two horizontal and two vertical wire chambers to determine the particle position and direction. The wire chambers were followed by a stack of three specially designed plastic scintillators. The first two scintillators allowed the determination of energy loss and remaining energy, which were used for particle identification. The third scintillator was a veto counter for $Z=1$ reaction products and was operated as a fast hardware veto to reduce dead time. Particles were also identified by TOF measurements using the time difference between the center plastic scintillator and the cyclotron RF.

It turned out that the ^8He from the ^{24}Si ground state were much more strongly forward peaked than expected from DWBA calculations. A measurement of level energies relative to the ground state is therefore not possible in the septum mode (minimum angle 4°) since the ground state was not visible. We subsequently developed operation in the transmission mode, where the primary α -beam is separated from the reaction products using the K600 spectrograph. While reaction products are detected in the medium dispersion focal plane, the α -beam is fed through a flange in the low dispersion focal plane and dumped in an external, well shielded cup. This allows measurements at 0° - 2° with a large solid angle of 4 msr (see Fig. 1).

We also found that excellent TOF discrimination is crucial for these low cross section (1 nb/sr) measurements. We therefore decided to run at a lower beam energy of 180 MeV, which allows cleaner beam-pulse selection.

The improved setup was tested in two additional runs in December 1995 and April 1996. These tests allowed us to improve shielding against background induced by the primary beam in the spectrometer and the external beam dump. We also developed the readout of the particle energy loss in the wire chambers, which is useful to discriminate particles further.

The 10-day production run was carried out in June 1996, concentrating mainly on measurements with the Si target. The K600 was operated in transmission mode at 1° . A beam current of 170 nA was found acceptable, being limited mainly by the radiation-induced leakage current in the vertical wire chambers. The internal resolution varied during the experiment from about 70 keV to 100 keV. The additional target contribution to the resolution is 110 keV for $^{28}\text{Si}(\alpha, ^8\text{He})$.

The ^8He position spectrum obtained from a 1.8 mg/cm^2 natural Si target after 40 h is shown in Fig. 2. The ground state of ^{24}Si can be clearly identified and is enhanced by at least two orders of magnitude compared to the measurements at 4.5° . Also clearly visible are the first two excited states at approximately the energies predicted by the shell model calculations. This is the first time that excited states in ^{24}Si have been measured.

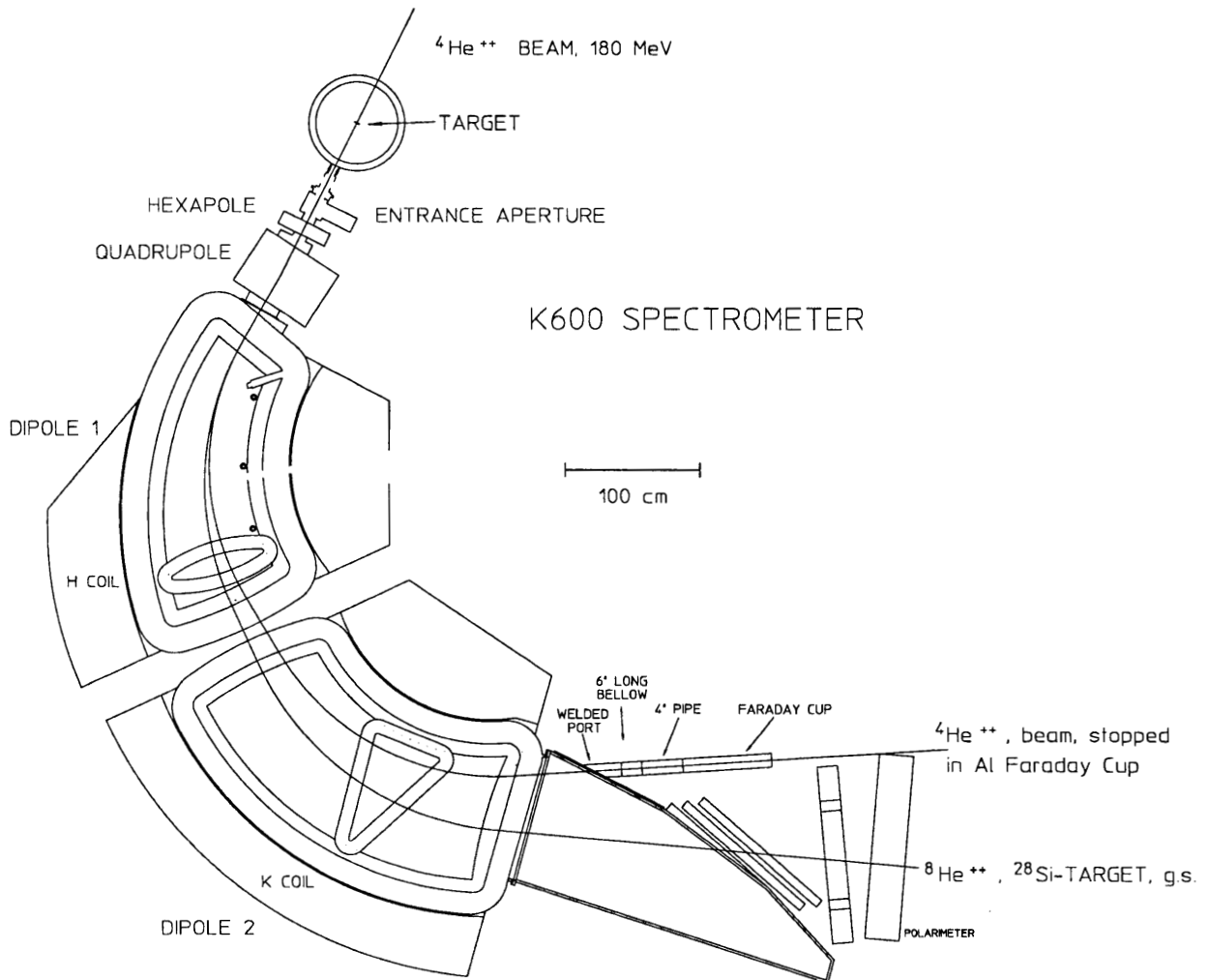


Figure 1. Setup for the K600 in transmission mode.

The second excited state is the first above the proton threshold and corresponds therefore to the resonance in the $^{23}\text{Al}(p,\gamma)^{24}\text{Si}$ cross section. The resulting reaction rate has to be determined when data analysis is completed.

An excellent focal plane calibration was obtained from the simultaneously measured ^6He position spectrum, originating from $(\alpha, ^6\text{He})$ reactions on ^{28}Si , ^{29}Si and ^{30}Si (see Fig. 2). Especially important are the calibration lines from ^{30}Si , since they are the only lines on the high momentum side of the excited ^8He states.

Two shifts were dedicated to measurements with ^{32}S targets. The main purpose was to determine the stability of the targets, which consisted of ^{32}S sandwiched between gold foils. The targets were stable for beam currents up to 120 nA, which makes them very suitable for this kind of experiments. In the ^8He position spectrum, the ^{28}S ground state can be clearly identified. Since the ^{28}S mass is uncertain,⁴ we expect to get from this

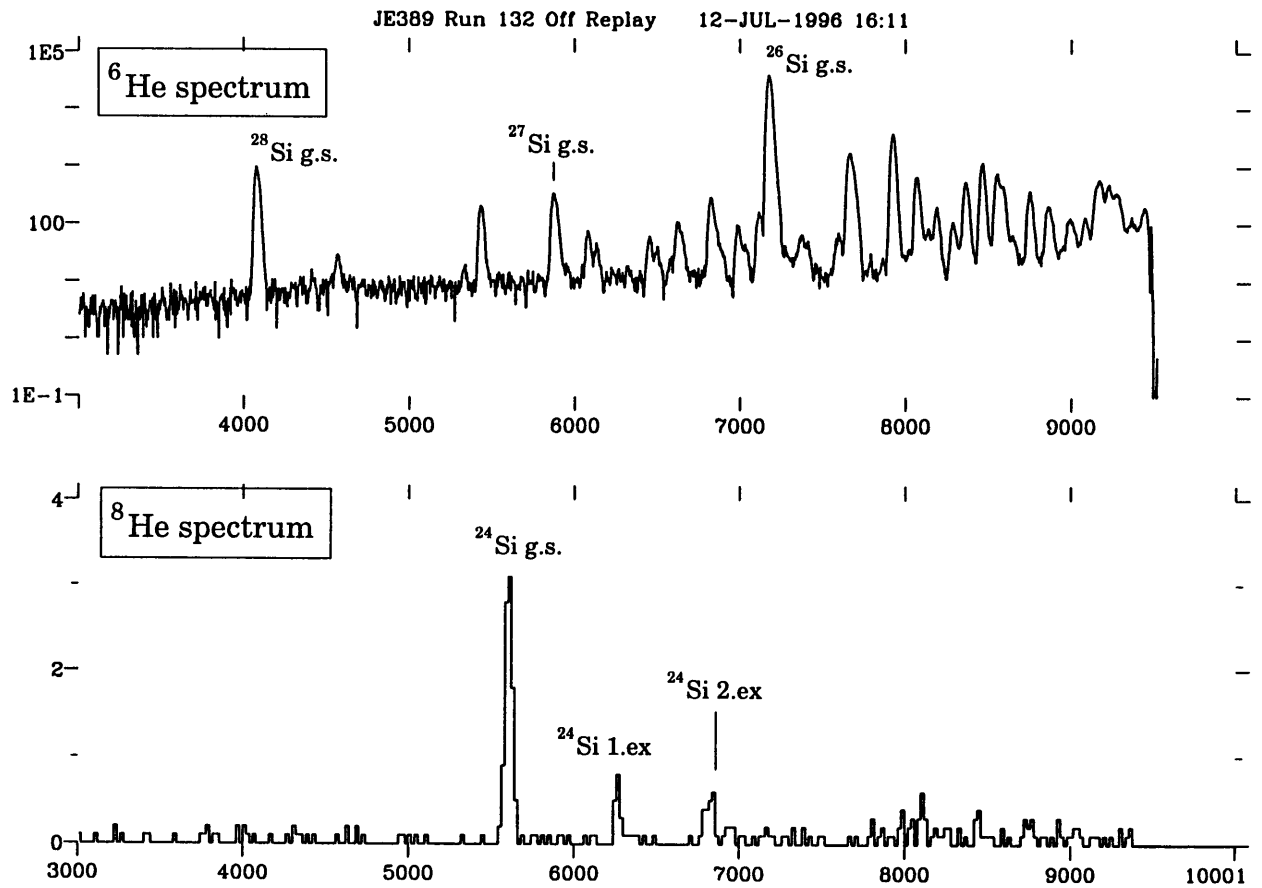


Figure 2. ${}^6\text{He}$ and ${}^8\text{He}$ position spectrum after approximately 40 h. In the ${}^6\text{He}$ spectrum only the ground states are labelled, though all the other states can be assigned to known excited states in ${}^{26}\text{Si}$, ${}^{27}\text{Si}$ or ${}^{28}\text{Si}$.

spectrum a greatly improved ${}^{28}\text{S}$ mass determination. The results demonstrate that the measurement of excited states in ${}^{28}\text{S}$ is possible with the current setup and corresponding experiments are planned for the future.

1. R.K. Wallace, S.E. Woosley, *Ap. J. Suppl.* **45**, 389 (1981).
2. L. VanWormer *et al.*, *Ap. J.* **432**, 326 (1994).
3. H. Herndl *et al.*, *Phys. Rev. C* **52**, 1078 (1995).
4. R.E. Tribble, D.M. Tanner, R.F. Zeller, *Phys. Rev. C* **22**, 17 (1980).